THE STRUCTURE OF SURFACE RHENIUM OXIDE ON ALUMINA FROM LASER RAMAN SPECTROSCOPY AND X-RAY ABSORPTION NEAR-EDGE SPECTROSCOPY

FRANKLIN D. HARDCASTLE, ISRAEL E. WACHS*

Zettlemoyer Center for Surface Studies, Departments of Chemical Engineering and Chemistry, Lehigh University, Bethlehem, PA 18015 (U.S.A.)

JOHN A. HORSLEY** and GRAYSON H. VIA

Corporate Research-Science Laboratories, Exxon Research and Engineering Company, Annandale, NJ 08801 (U.S.A.)

Summary

The interaction of rhenium oxide with an alumina support is examined over a wide range of conditions (rhenium oxide loading, calcination temperature and environment) using laser Raman spectroscopy (LRS) and X-ray absorption near-edge spectroscopy (XANES). These structural probes reveal that supported rhenium oxide on alumina is present as an atomically dispersed surface $[ReO_4]_{ads}$ species coordinated to the alumina support. The $[ReO_4]_{ads}$ species possesses C_{3v} symmetry which is consistent with the presence of three equivalent terminal Re—O bonds and one inequivalent Re—O bond as part of the Re—O—Al linkage to the alumina support. The $[ReO_4]_{ads}$ species are solvated by water molecules at ambient conditions, and the solvating water molecules readily desorb on heating in dry environments. The surface coverage of the $[ReO_4]_{ads}$ species declines with increasing calcination temperature, because the surface rhenium oxide species can apparently recombine in dry environments and elevated temperatures to yield gaseous dimeric Re_2O_7. Additional studies are required to determine if a $[Re_2O_7]_{ads}$ surface species can be isolated on the alumina support in dry environments and at high rhenium oxide surface coverages. The supported rhenium oxide on alumina system is dynamic, and the state of rhenium oxide depends on temperature, moisture/water content and rhenium oxide loading.

Introduction

Supported metal oxides occurring as two-dimensional surface metal oxides typically possess chemical and physical properties which differ

*Author to whom correspondence should be addressed.

**Present address: Catalytica Associates, Mountain View, CA, U.S.A.

0304-5102/88/$3.50

markedly from those of their unsupported metal oxide counterparts [1 - 11]. By varying experimental parameters (metal oxide surface coverage, calcination temperature and extent of hydration), the structures of both the surface metal oxide and the support can be affected. The different structures of the surface metal oxides, a consequence of their interactions with the support, usually modify the characteristic properties of the metal oxides. Direct monitoring of these different surface oxide structures by laser Raman spectroscopy (LRS) and X-ray absorption near-edge spectroscopy (XANES) yields vital information concerning the nature of the surface oxide/support interaction, since both techniques are highly sensitive to alterations in the coordination and molecular geometry of the surface metal oxide species. Rhenium oxide supported on alumina as a two-dimensional surface oxide has recently been the subject of numerous investigations [12 - 19]. To date, however, the structure of the surface rhenium oxide species remains a subject of debate.

Rhenium oxide supported on alumina has been investigated by a number of workers utilizing various instrumental techniques and sample preparations with the aim of ascertaining the structure of the surface rhenium oxide species [12 - 19]. *In situ* infrared (IR) studies by Olsthoorn and Boelhouwer monitored the characteristic vibrational bands of the surface hydroxyl groups of the alumina support possessing 195 $m^2 g^{-1}$ and concluded that complete monolayer coverage was achieved at ~20% Re/Al_2O_3 [12]. Although the surface metal oxide phase was not directly monitored, they proposed that the surface rhenium oxide consists of rhenium oxide aggregates on the alumina support. Yao and Shelef [13] examined low coverages of 1 - 4% Re/Al_2O_3 by electron paramagnetic resonance and temperature programmed reduction, and suggested the presence of rhenium oxide as both a two-dimensional, dispersed phase and a nondispersed phase which was characterized by different reduction temperatures. Kerkhof *et al.* [14] carried out the first laser Raman study of the supported rhenium oxide on alumina system at moderate loadings of 5 - 14% Re/Al_2O_3, and found the Raman spectra of the surface species to be consistent with a ReO_4^- species possessing tetrahedral symmetry. Nakamura *et al.* [15] examined 2 - 15% Re/Al_2O_3 by *in situ* IR and found the rhenium–oxygen stretching modes of the rhenium oxide species consistent with the perrhenate ion and crystalline Re_2O_7. Based on these observations, they suggested the presence of an adsorbed ReO_4^- species of tetrahedral symmetry at low coverages and an adsorbed dimeric Re_2O_7 species at higher coverages. Wang and Hall [16] studied 1 - 9% Re/Al_2O_3 and characterized the supported rhenium oxide by *in situ* laser Raman, IR and visible reflectance spectroscopies, and proposed a monomeric surface rhenium oxide species with distorted tetrahedral symmetry. Arnoldy *et al.* [17] recently suggested that a surface rhenium oxide phase is present for the rhenium oxide on alumina system from TPR studies. In contrast to previous evidence, Edreva-Kardjieva and Andreev [18] examined the rhenium oxide on alumina system under oxidative, precatalysis conditions by thermal analysis, diffuse

reflectance, XPS and IR, and suggested that the supported rhenium oxide is present as a monolayer of aluminum mesoperrhenate, $AlReO_5$.

X-ray absorption near-edge spectroscopy (XANES) and extended X-ray absorption and fine structure (EXAFS) measurements have also been carried out on the supported rhenium oxide on alumina system by Ellison *et al.* [19]. The measurements were made under ambient conditions on the Re L_3 edge for rhenium oxide on alumina catalysts prepared from ammonium perrhenate. They found that the EXAFS spectra of the high loading samples (10 and 15% Re/Al_2O_3), after calcining at 525 °C, resembled that of crystalline ammonium perrhenate, although some differences could be seen for the lower loading samples (2.5% Re/Al_2O_3). They concluded that at higher loadings the three-dimensional ammonium perrhenate structure was retained after calcination, but at low loadings surface rhenium oxide clusters were formed. A direct determination of the local geometry of the Re atom, however, was not made. It is, indeed, rather difficult to obtain details of the local geometry simply by inspection of the L_3 edge. A better edge for this purpose is the K or L_1 edge, which can be used to distinguish between a tetrahedral or octahedral environment.

It appears from these recent investigations of the supported rhenium oxide on alumina system that there is no clear model, illustrating the structure and nature of the surface rhenium oxide, which is consistent with the observations. The present study addresses the molecular structure of the surface rhenium oxide on alumina by examining a wide range of submonolayer rhenium oxide coverages on alumina using laser Raman spectroscopy and X-ray absorption near-edge spectroscopy (using the Re L_1 edge).

Experimental

The rhenium oxide on Al_2O_3 samples were prepared by impregnating γ-Al_2O_3, 180 $m^2\ g^{-1}$ (Harshaw), by the incipient wetness technique with a 60 - 70 wt.% aqueous solution of perrhenic acid, $HReO_4$ (Alfa). The samples were then dried for a few hours at room temperature, followed by drying for 18 h at 120 °C, and some samples were calcined at 500 °C for 16 h. The Re contents, as determined by X-ray fluorescence and ICP analysis, ranged from 0.1 - 20% Re/Al_2O_3 for samples dried at 120 °C and 0.1 - 13% Re/Al_2O_3 after calcination at 500 °C. Several samples were also calcined at 950 °C for 16 h to examine the effect of high temperature calcination.

The laser Raman experimental setup consists of an Ar^+ laser (Spectra Physics, Model 2020-05) delivering a cw beam of incident radiation tuned to 514.5 nm. The beam was focused onto the sample in a right-angle scattering geometry (illuminator: Spex, Model 1459) where the sample typically spins at about 2000 rpm (rotator: Spex, Model 1445A) to avoid local heating effects. The scattered light was then collected and directed into a Triplemate spectrometer (Spex, Model 1877) where the Raman signal is spatially separated as a function of frequency and detected by an inten-

sified photodiode array and optical multichannel analyzer (EG & G, Princeton Applied Research, Model 1463). The detector was thermoelectrically cooled to −30 °C. Data analysis was performed with the OMA III (EG & G) dedicated computer and software. The average resolution obtained was experimentally determined to be about 2 cm^{-1} where a spectral region of about 800 cm^{-1} was simultaneously collected. Additional details concerning the optical arrangement of the Raman apparatus may be found in [20].

The X-ray absorption data were obtained at the Stanford Synchrotron Radiation Laboratory (SSRL) on beamline VII-3 during dedicated operation of SPEAR at 3 GeV and currents of 30 - 80 mamp. Data for air-exposed samples were taken at room temperature using apparatus designed for transmission and fluorescence X-ray spectroscopy [21, 22]. The fluorescence detector was similar to that described by Stern and Heald [23]. Data were also taken on samples after *in situ* calcination at 500 °C in a mixture of 20% oxygen in helium in order to investigate the effect of removal of the surface-coordinated water. The measurements were carried out *in situ* at 500 °C and at room temperature, without exposing the samples to ambient air. For these experiments an *in situ* catalyst furnace designed for simultaneous transmission and fluorescence measurements was used [24].

Results

Raman spectroscopy

Raman spectra of transition metal oxide compounds can yield detailed information with regard to their local molecular structures. This is also true for transition metal oxides present as two-dimensional supported metal oxides [20]. The local geometry of the surface metal oxide may be determined by utilizing vibrational mode analysis [25] and by comparison of the Raman spectra of the supported metal oxides of unknown structure with the spectra of compounds possessing established structures (reference compounds). The Raman spectra of several bulk rhenium oxide reference compounds and the supported rhenium oxide on alumina samples are presented below.

Rhenium oxide reference compounds

The molecular geometry of a two-dimensional surface metal oxide species, as determined by Raman spectroscopy, can best be described in terms of vibrational mode analysis. For an undistorted tetrahedral molecule (point group T_d) of type ReO_4, four fundamental modes of vibration are possible, $A_1 + E + F_2 + F_2$, and all four are Raman active [26]. As the ReO_4 tetrahedron is distorted and the point symmetry lowered (*i.e.* to C_{3v}, C_{2v}, etc.), a greater number of the nine possible fundamental vibrational modes ($3N - 6$ for a nonlinear, polyatomic molecule) become active, resulting in a more complicated Raman spectrum.

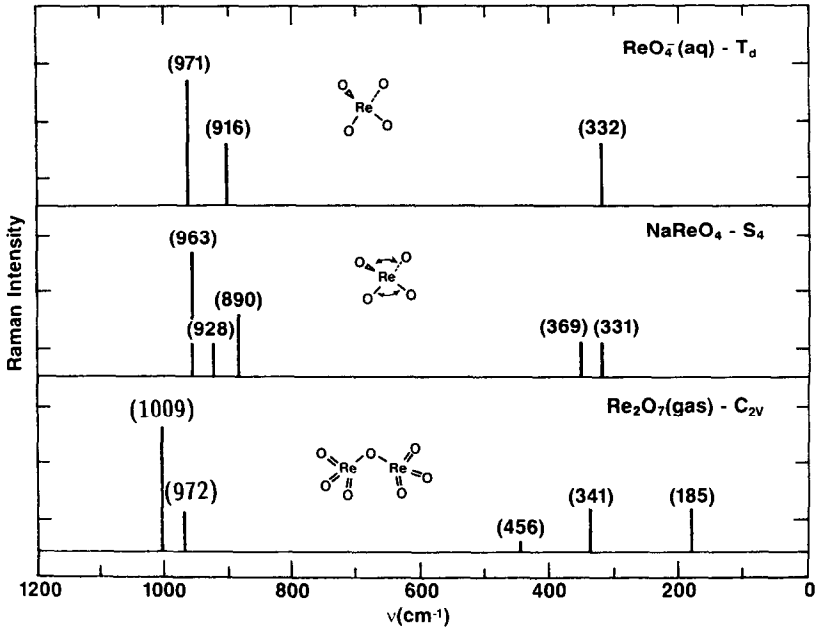

Fig. 1. Stick diagrams representing the Raman spectra of tetrahedrally coordinated rhenium oxide compounds ReO_4^-(aq), $NaReO_4$ and Re_2O_7(gas).

A perfect ReO_4-type tetrahedron is exemplified by the perrhenate ion in aqueous solution, ReO_4^-(aq) [27], and its Raman spectrum is represented at the top of Fig. 1 as a stick diagram. The rhenium–oxygen vibrations show a symmetric stretch at 971 cm^{-1}, an antisymmetric stretch at 916 cm^{-1}, and two bending modes or deformations which are degenerate in frequency at 332 cm^{-1}. The symmetry of a tetrahedrally coordinated molecule confined to a crystalline lattice is generally lower than T_d, since molecular distortions occur in order to accommodate the lattice structure. For example, the scheelite-type crystal structure of $NaReO_4$ imposes S_4 site symmetry on the ReO_4 tetrahedron [28]. A stick diagram representing the Raman spectrum of $NaReO_4$ is shown in Fig. 1 for comparison with that for the ideal tetrahedral perrhenate ion [28]. As expected, the lower symmetry present in $NaReO_4$ results in a more complicated Raman spectrum: the antisymmetric stretching mode has split into two peaks at 928 and 890 cm^{-1}, and the degeneracy of the bending modes has been lifted, giving rise to peaks at 369 and 331 cm^{-1}.

Octahedrally coordinated molecules of type ReO_6 (point group O_h) ideally possess only three Raman-active modes, $A_{1g} + E_g + F_{2g}$, from a total of fifteen possible vibrational modes (3N − 6) [25]. Ideal ReO_6-type octahedra are rare, but an example is found in the compound α-Li_6ReO_6 for which the Raman spectrum is represented at the top of Fig. 2 [29]. Only the three fundamental modes characteristic of the ideal octahedron are

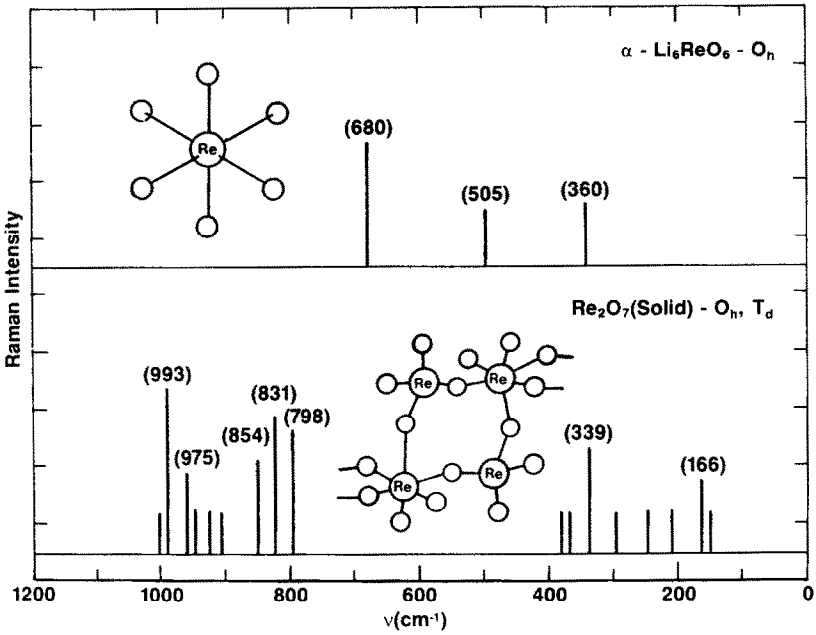

Fig. 2. Stick diagrams representing the Raman spectra of octahedrally coordinated rhenium oxide compounds α-Li_6ReO_6 and Re_2O_7(solid).

active for α-Li_6ReO_6 [29]: 680 cm^{-1} (A_{1g}), 505 cm^{-1} (E_g) and 360 cm^{-1} (F_{2g}). As distortions are imposed on the ReO_6 group and the symmetry is lowered (*i.e.* D_{4h}, D_{2h}, D_{3d}, etc.), a greater number of the fifteen possible fundamental modes would be expected to become Raman active [25].

The symmetric rhenium–oxygen stretching mode (the so-called 'breathing' mode), is typically the Raman band of greatest intensity and the highest in frequency. This band reflects the greatest bond order present in the molecule and often gives some indication of the coordination of the central metal atom. For example, the trend in symmetric rhenium–oxygen stretching frequencies for the barium salts of the ReO_6, ReO_5 and ReO_4 groups are 622, 700 and 980 cm^{-1}, respectively [30]. This trend reflects the decreasing coordination of the central rhenium atom and a change in molecular geometry from octahedral to tetrahedral for the rhenium oxide. The Raman spectra shown in Figs. 1 and 2 for the rhenium oxide reference compounds demonstrate how laser Raman spectroscopy can directly discriminate between rhenium oxide compounds possessing octahedral or tetrahedral structures.

Raman spectroscopy also allows discrimination between monomeric and polymeric metal oxide species. In general, for molecules in similar environments, the polymeric species possess a higher terminal metal–oxygen bond order, which results in a higher symmetric metal–oxygen stretching frequency. Additional characteristic Raman features appear for the poly-

meric species depending on whether the metal–oxygen–metal linkages, M—O—M, are linear or bent. Generally, for rhenium oxide compounds with linear Re—O—Re linkages the antisymmetric and symmetric stretching frequencies for this three-body functionality occur at ≈720 - 860 cm^{-1} and ≈200 - 205 cm^{-1}, respectively [31]. The vibrational frequencies for the bent Re—O—Re system are best portrayed by gaseous Re_2O_7 [32], shown in Fig. 1, where the Re—O—Re stretching modes occur at ≈800 cm^{-1} (antisymm.) and ≈456 cm^{-1} (symm.), and the bending mode at ≈185 cm^{-1}. The Raman intensity of the antisymmetric stretching mode at ≈800 cm^{-1} is very weak, but can be easily observed by IR spectroscopy. These characteristic Raman bands for the Re—O—Re functionality are unique, and serve as a set of group-frequency band assignments for the identification of polymeric rhenium oxide chains (containing Re—O—Re linkages) in various types of rhenium(VII) oxide systems.

The dirhenium heptoxide molecule Re_2O_7 or $O_3Re—O—ReO_3$, is composed of two tetrahedral ReO_3 units bridged by a common oxygen atom via a bent Re—O—Re linkage. The molecular geometry of this dimeric species in both the liquid and gas phases is quite similar, and the two phases exhibit nearly identical Raman spectra [32]. This geometry closely resembles that of the aqueous dichromate ion, $Cr_2O_7^{2-}$(aq), and is reported to belong to the same molecular point group, C_{2v}. The stretching modes of the terminal Re—O groups occur at 1009 and 972 cm^{-1}, as depicted in Fig. 1, shifted to higher frequency from the values of the ideal ReO_4 tetrahedron (perrhenate ion) as a consequence of the increased terminal Re—O bond order of the dimer compared to the monomer. The bending mode is found to be shifted from 332 to 341 cm^{-1}. Dirhenium heptoxide also exhibits vibrational modes characteristic of the bent Re—O—Re linkage. Two prominent bands occur at 456 and 185 cm^{-1} which are assigned to the symmetric Re—O—Re stretching and bending modes, respectively, and a very weak antisymmetric Re—O—Re stretch is observed at 800 cm^{-1}.

The structure of crystalline Re_2O_7 consists of both octahedral ReO_6 and tetrahedral ReO_4 units linked by oxygen bridges to complete a polymeric chain structure of double layers [32]. The weak van der Waals forces between the double layers give rise to complicated splitting patterns of the fundamental Raman bands, and are characteristic of the crystalline Re_2O_7 lattice. Figure 2 shows that the high-frequency region of the Raman spectrum, 798 - 1008 cm^{-1}, consists primarily of the terminal Re—O stretching modes while the low-frequency region, 100 - 400 cm^{-1}, consists of Re—O bending modes and Re—O—Re stretching and bending modes. The bands near 993 and 975 cm^{-1} are probably due to the tetrahedrally coordinated members of the crystalline polymeric chain, while the bands near 854, 831 and 798 cm^{-1} result from the octahedrally coordinated members. The antisymmetric Re—O—Re stretch is expected near 800 cm^{-1}, but should be of very weak intensity; the corresponding Re—O—Re bending mode is observed at 166 cm^{-1} (compare with the Re—O—Re bending mode of the tetrahedral dimer, Re_2O_7 (liquid or gas), at 185 cm^{-1}).

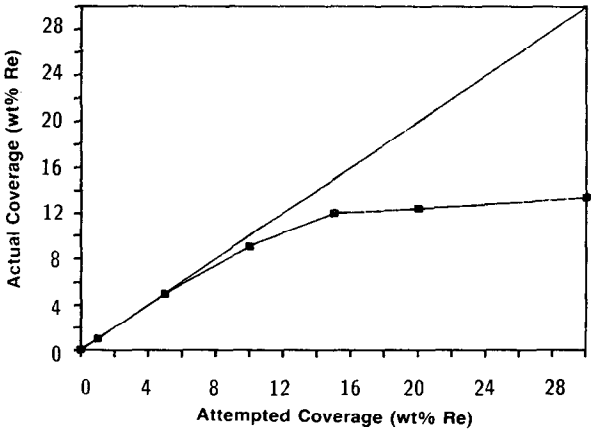

Fig. 3. Attempted coverage (during impregnation) plotted *versus* actual coverage (after calcination at 500 °C) for Re/Al_2O_3 samples.

Rhenium oxide supported on alumina

A range of rhenium oxide coverages were attempted on the alumina support which should have resulted in 0.1 - 30 wt.% Re/Al_2O_3. However, only 0.1 - 13 wt.% Re/Al_2O_3 remained after calcination at 500 °C. The quantitative relationship of 'actual' *versus* 'attempted' coverages is graphically illustrated in Fig. 3. A linear relationship is observed for attempted coverages of less than 10% Re/Al_2O_3, but asymptotically approaches ~13% Re/Al_2O_3 as higher coverages are attempted. The 10% Re/Al_2O_3 sample retained 9% of its original rhenium content, the 15% and 20% samples retained ~12% rhenium, and the sample prepared as 30% Re/Al_2O_3 retained only 13% of its original rhenium content after calcination at 500 °C. The value of 13% Re/Al_2O_3 is apparently a 'saturation limit' for the amount of rhenium oxide capable of remaining on the alumina support for Re/Al_2O_3 samples calcined at 500 °C for 16 h. The amount of rhenium lost is a function of both initial rhenium content and calcination temperature, since the sample prepared as 30% Re/Al_2O_3 showed a decrease to 20% Re/Al_2O_3 after drying at 120 °C and a further decrease to 13% Re/Al_2O_3 after calcination at 500 °C. Thus, these samples will be referred to as 9%(10%) Re/Al_2O_3 (500 °C), 12%(15%) Re/Al_2O_3 (500 °C), 12%(20%) Re/Al_2O_3 (500 °C), 13%(30%) Re/Al_2O_3 (500 °C) and 20%(30%) Re/Al_2O_3 (120 °C), where the first number refers to the actual rhenium content and the number in parentheses refers to the rhenium content employed during impregnation.

The Raman spectra for a 20%(30%) Re/Al_2O_3 (120 °C) sample (prepared as 30% Re/Al_2O_3 and dried at 120 °C) and an aqueous perrhenate solution are shown in Fig. 4 for comparison. The Raman band positions for the ReO_4^-(aq) solution occur at 971 (sym. stretch), 916 (antisym. stretch) and 332 cm^{-1} (bending). The Raman bands of 20%(30%) Re/Al_2O_3 (120 °C) are very similar to those of the aqueous perrhenate ion, which exhibit the

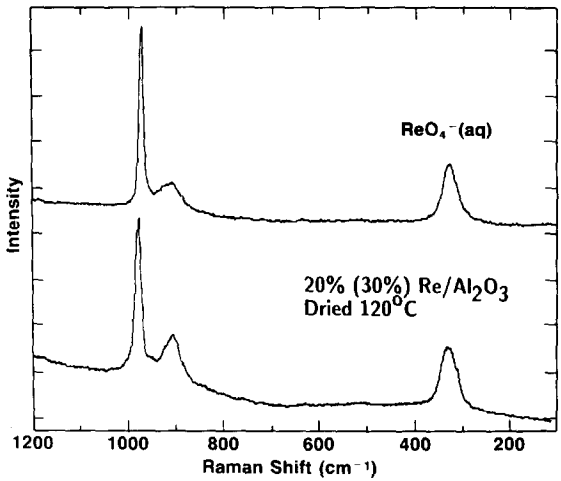

Fig. 4. Raman spectra of the aqueous perrhenate ion (top) and of a 20%(30%) Re/Al_2O_3 sample dried at 120 °C (bottom).

same modes at slightly different locations, *viz.* 982, 916 and 332 cm^{-1}, respectively. The observed 11 cm^{-1} shift of the symmetric Re—O stretch to a higher wavenumber reflects the different environments of the ReO_4^- ion in aqueous solution, compared to the species supported on the alumina surface. The Raman vibrational features are quite similar, however, for the ReO_4^- ion in these two very different environments, suggesting similar molecular geometries for both the aqueous perrhenate ion and the surface rhenium oxide species supported on alumina. Furthermore, the surface rhenium oxide species appears to be isolated on the alumina surface, as indicated by the absence of bands at ≈800, ≈450 and ≈200 cm^{-1} which are characteristic of Re—O—Re linkages.

A series of Raman spectra were collected under ambient conditions for the rhenium oxide on alumina system as a function of rhenium oxide content, 1 - 13%(1 - 30%) Re/Al_2O_3 (500 °C), and are shown in Fig. 5. The Raman band positions for the supported rhenium oxide species occur at 982, ≈920 and 332 cm^{-1}. These band positions and the relative intensities remain unaltered from low to high coverages. From the above discussion concerning the correlation of Raman vibrational modes with structure for the rhenium oxide standards (Figs. 1, 2 and 4), it is clear that the spectra of Fig. 5 are consistent with an isolated $[ReO_4]_{ads}$ surface species. Furthermore, since the relative band intensities and frequency locations do not change with coverage, neither does the molecular geometry of the rhenium oxide surface species. Therefore, the above findings are consistent with an isolated $[ReO_4]_{ads}$ surface species with a structure which is independent of surface coverage.

Previous *in situ* laser Raman studies have demonstrated that water molecules coordinate to two-dimensional supported metal oxide phases and

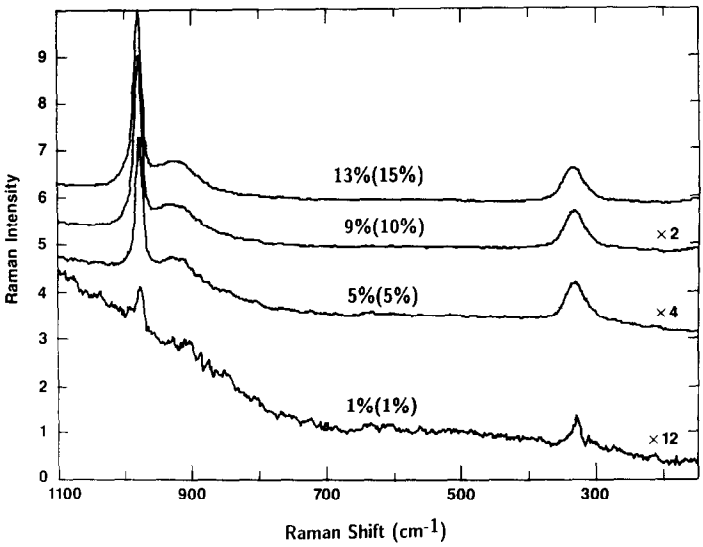

Fig. 5. Raman spectra of a series of rhenium oxide on alumina samples at sub-monolayer coverages, 1 - 13% Re/Al_2O_3, calcined at 500 °C.

decrease the metal–oxygen bond order [5, 11, 16, 20, 33, 34]. The terminal metal–oxygen stretching frequency is decreased by an amount commensurate with the degree of water coordination or hydration. Thus, water adsorption can be used as a probe to aid in the determination of whether or not a particular supported metal oxide phase is present as a two-dimensional surface oxide species *adsorbed* on the alumina surface [20]. In contrast, a two-dimensional metal oxide species *absorbed* or incorporated into the subsurface region of the alumina support would not be affected by the presence of water vapor, since these species are inaccessible to the water molecules present on the surface [20, 35].

Laser-induced dehydration experiments [36] were performed on the 12%(15%) Re/Al_2O_3 (500 °C) sample under ambient conditions to examine the effect of moisture on the vibrational spectrum of the rhenium oxide on alumina system, and the Raman spectra are presented in Fig. 6. The relative temperature of the probed surface region was controlled by altering the power of the incident laser beam and the rate at which the sample was spinning. For a sample wafer (16 mm diameter), rotating at about 2000 rpm, the symmetric Re—O stretch occurs at 982 cm^{-1} under 80 mW incident laser power. This band increases in frequency to 1012 cm^{-1} for the sample held stationary under 214 mW incident laser power, due to the thermal desorption of the coordinated water molecules. This 30 cm^{-1} shift to higher frequency is due to an increase in the rhenium–oxygen bond order and a decrease in the extent of hydration for the supported rhenium oxide species on the alumina surface. This behavior is reversible, as demonstrated by a gradual shift of the Raman band from 1012 cm^{-1} back to 982 cm^{-1} under

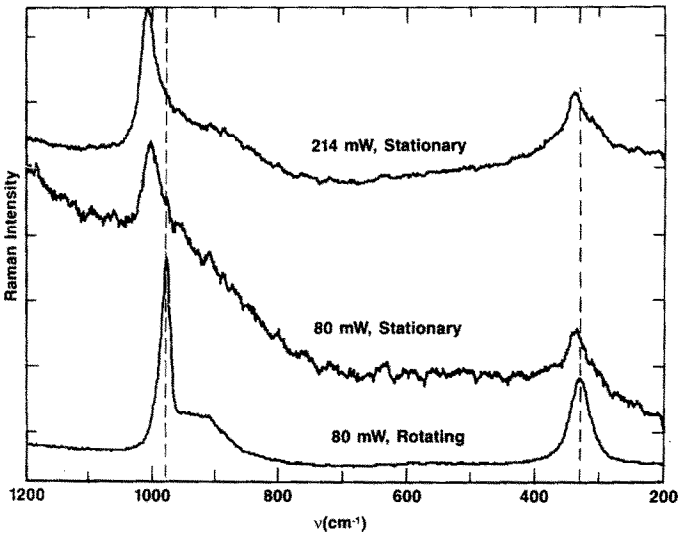

Fig. 6. Raman spectra showing effect of laser-induced dehydration on Re—O bond order for 12%(15%) Re/Al_2O_3 (500 °C) sample.

low laser power when moisture returns to the probed surface. The antisymmetric Re—O stretch thermally broadens under laser-induced dehydration, and the bending mode at 332 cm^{-1} increases in peak position by about 10 cm^{-1}. The effects of laser-induced dehydration on the rhenium oxide supported on alumina system demonstrate that the surface rhenium oxide species is present as a two-dimensional surface phase *adsorbed* on the alumina support surface.

The influence of calcination temperature upon the rhenium oxide supported on alumina system was also investigated, and the effects of calcining a 10% Re/Al_2O_3 (120 °C) sample at 500 °C and at 950 °C for 16 h are presented in the Raman spectra of Fig. 7. Ninety percent of the original rhenium was retained by the sample after calcining at 500 °C, resulting in a 9%(10%) Re/Al_2O_3 (500 °C) sample. A 3%(10%) Re/Al_2O_3 (950 °C) sample resulted after calcining the 9%(10%) Re/Al_2O_3 (500 °C) sample at 950 °C for 16 h. During the 950 °C calcination, the surface area of the alumina decreased from 180 to 65 $m^2\ g^{-1}$ and the alumina support phase-transformed from γ-Al_2O_3 to δ- and θ-Al_2O_3. The γ-Al_2O_3 phase exhibits a relatively flat background Raman spectrum but the δ- and θ-Al_2O_3 structures do exhibit several Raman features below 850 cm^{-1} [20]. The bands resulting from δ- and θ-Al_2O_3 have been subtracted from the Raman spectrum of 3%(10%) Re/Al_2O_3 (950 °C) and the modified spectrum is shown together with that of the 9%(10%) Re/Al_2O_3 (500 °C) sample in Fig. 7. There are no significant shifts or changes in the relative intensities of the Raman bands for the supported rhenium oxide between calcination at 500 °C and 950 °C, suggesting that no apparent change occurred in the structure of the surface rhenium

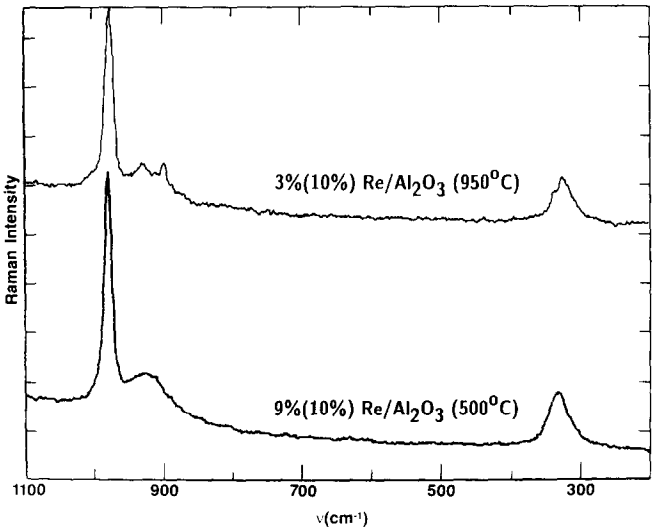

Fig. 7. Raman spectra of 9%(10%) Re/Al_2O_3 (500 °C) and 3%(10%) Re/Al_2O_3 (950 °C) showing the effects of calcination temperature on the Raman bands, thus demonstrating the stability of rhenium oxide on alumina at elevated temperatures. The δ,θ-Al_2O_3 Raman bands were subtracted from the 950 °C spectrum.

oxide on the alumina support. Many of the surface hydroxyl groups, which are sources of both background fluorescence and surface non-uniformity, are removed by the 950 °C treatment and a better-resolved Raman spectrum is obtained for this sample [37, 38]. The splitting of the antisymmetric Re—O stretch (≈920 cm^{-1}) into a doublet at 931 and 902 cm^{-1}, and the bending modes (332 cm^{-1}) at 360 and 336 cm^{-1}, yield additional information concerning the type of distortion imposed on the $[ReO_4]_{ads}$ species. A tetrahedrally coordinated rhenium oxide species possessing C_{3v} symmetry (*i.e.* one oxygen atom is inequivalent to the remaining three oxygen atoms) is consistent with the splitting of the antisymmetric stretch into a doublet, $F_2 \rightarrow A_1 + E$, and the splitting of the bending mode into a doublet, $F_2 \rightarrow A_1 + E$ [24]. Thus, the $[ReO_4]_{ads}$ surface species on the alumina support possesses C_{3v} symmetry under ambient conditions.

In order to determine the ease of hydrolysis of the surface rhenium oxide bond from the alumina support (Re—O—Al linkage), several 1 g samples of 12%(15%) Re/Al_2O_3 (500 °C) were rinsed with 100 cm^3 of hot or cold water. There was no significant difference in the amount of rhenium oxide extracted between the hot and cold rinses. Approximately 8% Re remained on the surface as a surface oxide, as determined by X-ray fluorescence, and roughly one-third of the starting surface oxide was washed from the surface as the perrhenate ion, ReO_4^-(aq). Raman spectroscopy was used to monitor the chemical state of the surface rhenium oxide on alumina before and after washing. No changes in Raman peak positions or relative intensities resulting from the rinsing treatments were detected.

XANES

X-ray absorption near-edge spectroscopy (XANES) provides a means of investigating the symmetry of the local environment around a given atom. At the K (or L_1) absorption edge in transition metal compounds, a pre-edge feature is often observed, arising from a transition from the 1s (or 2s) core orbital to an orbital of predominantly metal d character. If there is a center-of-inversion symmetry at the transition metal (*e.g.* octahedral ligand environment), then the transition is dipole-forbidden and no pre-edge feature is observed. If there is no center-of-inversion symmetry (*e.g.* tetrahedral ligand environment), some metal p-orbital character is mixed into the upper state, resulting in a dipole-allowed transition and a pre-edge feature. Figure 8 shows the Re L_1 edge region in the model compounds NH_4ReO_4, where the Re has a tetrahedral environment, and ReO_3, where the Re is bonded to six oxygens in a regular octahedral configuration. There is a fairly intense pre-edge feature in the tetrahedral NH_4ReO_4 spectrum which is completely absent in the octahedral ReO_3 spectrum. Distortion of a regular octahedral environment removes the center-of-inversion symmetry and allows some p character to be mixed into the upper state. However, the resultant pre-edge feature is usually of much lower intensity than that produced by a tetrahedral environment and generally appears as a small shoulder on the rising absorption edge [39].

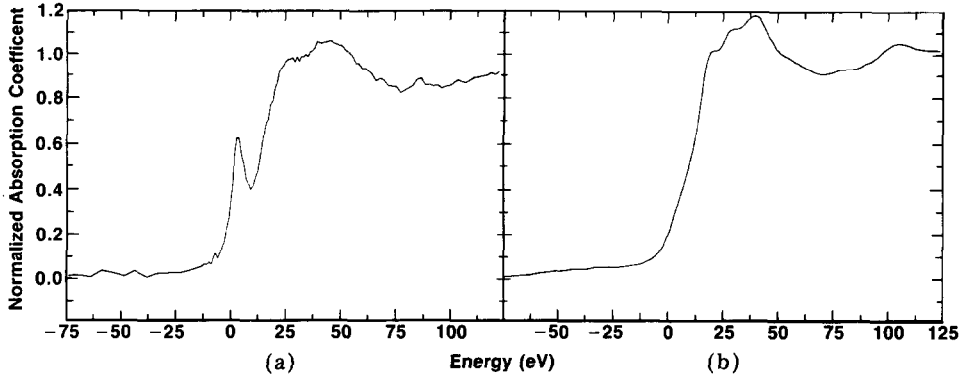

Fig. 8. XANES spectra showing the Re L_1 edge region for the model compounds (a) NH_4ReO_4 and (b) ReO_3.

The Re L_1 edge spectra for 1%(1%) and 12%(15%) Re/Al_2O_3 (500 °C), air-exposed and at room temperature, are shown in Fig. 9. The two spectra are very similar, showing that there is little change in structure as the loading is increased. A very similar XANES spectrum was also obtained for 0.1%(0.1%) Re/Al_2O_3. The XANES spectra of the air-exposed rhenium oxide supported on alumina closely resemble the XANES spectrum of the NH_4ReO_4 model compound, indicating that for the surface rhenium oxide species the Re environment is close to tetrahedral under these conditions. The intensity of the pre-edge feature is somewhat lower in the spectra of

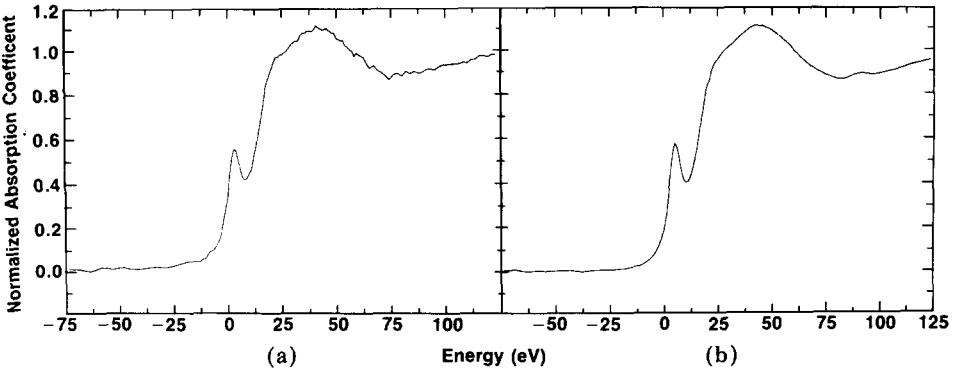

Fig. 9. XANES spectra showing the Re L_1 edge region for (a) 1%(1%) and (b) 12%(15%) Re/Al_2O_3 (500 °C) samples which were air-exposed (wet) and at room temperature.

the supported rhenium oxide on alumina samples than in the spectrum of the NH_4ReO_4 model compound.

In situ XANES measurements were also performed on the Re L_1 edge of 1%(1%) Re/Al_2O_3 (500 °C) by heating the sample to 400 °C in dry $He–O_2$. The XANES spectrum is presented in Fig. 10. The intensity of the pre-edge feature is further lowered somewhat by the *in situ* treatment. The XANES spectrum remained constant under *in situ* conditions between room temperature and 400 °C, and underwent a slight increase in the pre-edge feature upon exposure to ambient air, which contains moisture, at room temperature.

Discussion

The Raman and X-ray absorption near-edge spectroscopy results demonstrate that the surface rhenium oxide species on alumina are present as $[ReO_4]_{ads}$ units under ambient conditions. Comparison of the Raman spectra of the rhenium oxide supported on alumina samples with reference rhenium oxide compounds clearly reveals the similarity between the surface rhenium oxide species on alumina and isolated ReO_4-containing compounds (see Figs. 1, 2 and 5). The $[ReO_4]_{ads}$ species are isolated on the alumina surface at ambient conditions because they do not possess Re—O—Re linkages (characteristic bending mode at ≈160 - 200 cm^{-1}). The presence of $[ReO_4]_{ads}$ species on alumina is further supported by XANES measurements, which depict similar XANES features for the surface rhenium oxide species on alumina at ambient conditions and for the reference rhenium oxide compounds containing ReO_4 groups (see Figs. 8 and 9). The Raman and XANES features do not vary with the rhenium oxide coverage, and reveal that the surface rhenium oxide structure under ambient conditions does not change with rhenium oxide coverage. Thus, rhenium oxide–rhenium oxide interactions must be weak, and the rhenium oxide–alumina inter-

actions do not appear to be dependent on rhenium oxide surface coverage under ambient conditions.

The symmetry of the $[ReO_4]_{ads}$ surface species on alumina is also contained in the Raman spectra of the supported rhenium oxide on alumina. The non-uniform nature of the γ-Al_2O_3 surface calcined at 500 °C gives rise to very broad Raman bands which hinder symmetry analysis of the $[ReO_4]_{ads}$ species [37]. Calcination at 950 °C, however, transforms γ-Al_2O_3 to δ- and θ-Al_2O_3 which possess a more uniform surface [39]. All the Raman features of the $[ReO_4]_{ads}$ species are readily resolved after calcination at 950 °C (see Fig. 7), and reveal that the $[ReO_4]_{ads}$ species possess C_{3v} symmetry. The C_{3v} symmetry is consistent with the presence of three equivalent terminal Re—O bonds and one inequivalent Re—O bond as part of the Re—O—Al linkage to the alumina support. The Re—O—Al linkage is easily hydrolyzed in the presence of water, since a significant portion of the $[ReO_4]_{ads}$ can be washed from the alumina surface.

Additional information about the chemical state of the $[ReO_4]_{ads}$ species on alumina is obtained from laser-induced dehydration experiments. The laser-induced dehydration studies reveal that the $[ReO_4]_{ads}$ species are solvated by water molecules at ambient conditions and that the solvating water molecules can be thermally desorbed by mildly heating the sample (see Fig. 6). The ability of the adsorbed water molecules to alter the vibrational modes of the $[ReO_4]_{ads}$ species demonstrates that the surface rhenium oxide species on alumina are present as a two-dimensional surface phase adsorbed on the alumina support surface. The maximum amount of rhenium oxide present on the alumina support after calcination at 500 °C is also consistent with the presence of a two-dimensional surface rhenium oxide layer. A complete monolayer of surface rhenium oxide on the Al_2O_3 support containing 180 $m^2\ g^{-1}$ should correspond to $\approx$18 · 20% Re/Al_2O_3 by analogy with a monolayer of tungsten oxide on the same support [39]. The maximum loading of rhenium oxide on alumina achieved in the present study was only $\approx$13 wt.% Re/Al_2O_3 at 500 °C, which is significantly less than a complete monolayer (see Fig. 3). The ability of the $[ReO_4]_{ads}$ species to recombine and desorb as gaseous dimeric Re_2O_7 molecules at high surface coverages and elevated temperatures most probably accounts for the difficulty in achieving a close-packed monolayer of the surface rhenium oxide species on alumina.

The changes observed with Raman spectroscopy are also reflected in the X-ray absorption near-edge spectroscopy measurements. The intensity of the XANES pre-edge feature has previously been found to correlate strongly with the size of the molecular 'cage' defined by the first shell of ligands. The cage potential confines the upper state orbital in the vicinity of the adsorbing atom, and the smaller the cage the higher the oscillator strength of transitions to the orbital. Kutzler *et al.* [40] found a strong correlation between the bond length and the intensity of the pre-edge feature in the chromate, molybdate and thiomolybdate ions, and Wong *et al.* [41] found that the intensity of the pre-edge feature in a series of vanadium com-

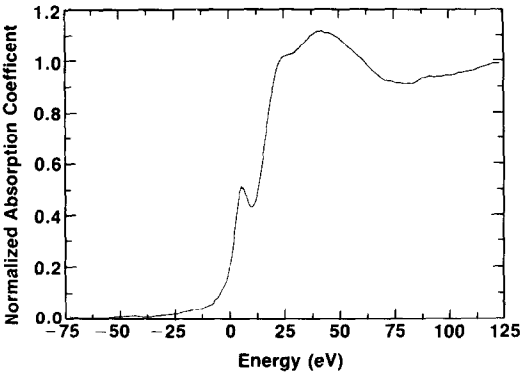

Fig. 10. XANES spectrum showing the Re L_1 edge region for 1%(1%) Re/Al_2O_3 (500 °C) *in situ* (dry) after heating to 400 °C.

pounds was very sensitive to the average bond length of the nearest neighbors. The average bond length in the surface rhenium oxide species may be slightly longer than the Re—O bond length in NH_4ReO_4, resulting in a pre-edge feature of somewhat lower intensity (see Figs. 8 and 9). A further increase in bond length may take place upon dehydration of the surface species (see Fig. 10). The intensity of the pre-edge feature is somewhat lower for the *in situ*, 'dry' sample than the pre-edge intensity for the 'wet' samples. This may reflect a change in average metal–ligand bond length due to the distortion of the surface species to C_{3v} symmetry and the formation of a bond between the surface species and the alumina support. An increase in the coordination of a small percentage of surface rhenium atoms from tetrahedral to octahedral coordination, as the surface water molecules are removed, would also be consistent with an increase in the average rhenium–oxygen bond length and cannot be ruled out.

The Raman and X-ray absorption near-edge spectroscopy findings suggest the following model for the supported rhenium oxide on alumina system:

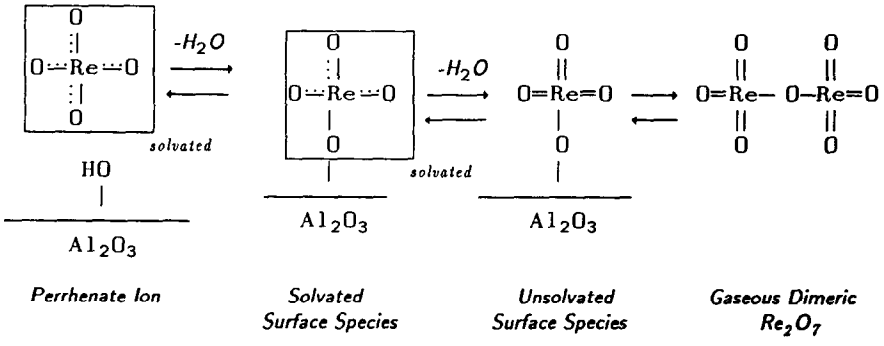

In aqueous solution rhenium oxide is present as the perrhenate ion, ReO_4^-(aq), which possesses the tetrahedral rhenium–oxygen symmetric stretch at 971 cm^{-1}. The perrhenate ion interacts with the alumina support by displacing the surface hydroxyl and coordinating directly to the alumina substrate [12]. The coordinated $[ReO_4]_{ads}$ species remains solvated by water molecules and possesses C_{3v} symmetry due to the formation of the Re—O—Al linkage. The distortion from ReO_4^-(aq) to solvated $[ReO_4]_{ads}$ increases the rhenium–oxygen symmetric stretch from 971 to 982 cm^{-1} and reflects the increase in average rhenium–oxygen bond order. The solvating water molecules can be thermally removed from the sample in dry environments. The removal of the solvating water molecules causes a further distortion of the $[ReO_4]_{ads}$ species, which increases the rhenium–oxygen symmetric stretch from 982 to 1012 cm^{-1}, reflecting a further increase in the average rhenium–oxygen bond order. The unsolvated $[ReO_4]_{ads}$ species apparently possesses the ability to surface diffuse, recombine and desorb from the alumina surface as the gas-phase, dimeric Re_2O_7 molecule at elevated temperatures. All of the above processes are reversible, since gaseous, dimeric Re_2O_7 molecules can be adsorbed onto an alumina surface to form the $[ReO_4]_{ads}$ species [12]. Exposure to moisture results in solvation of the $[ReO_4]_{ads}$ species (decrease in the rhenium–oxygen symmetric stretch from 1012 to 982 cm^{-1}), and rinsing with water hydrolyzes the Re—O—Al bond to yield the aqueous perrhenate ion, ReO_4^-(aq) (decrease in the rhenium–oxygen symmetric stretch from 982 to 971 cm^{-1}). A stable, dimeric $[Re_2O_7]_{ads}$ surface species on the alumina support was not observed in the present investigation, but cannot be completely ruled out on the basis of laser-induced dehydration experiments, performed in the presence of ambient moisture which easily hydrolyzed the Re—O—Re bond [24, 25].

Previous investigations of the rhenium oxide supported on alumina system have given rise to various models, but a unifying model describing this system on a molecular level has not been achieved [12 - 19]. These different conclusions developed as a consequence of comparing data from air-exposed and *in situ* measurements, the use of widely different experimental techniques, experimental artifacts, and conclusions that were not rigorously derived from the available experimental data. The early *in situ* IR spectroscopic studies of Olsthoorn and Boelhouwer monitored only the alumina surface hydroxyl groups and did not obtain any direct information on the state of the supported rhenium oxide phase [12]. These investigators, nevertheless, proposed that rhenium oxide aggregates were present on the alumina support. Rhenium oxide aggregates, if present, would be expected to possess significant Re—O—Re linkages (strong Raman bending modes in the 160 - 200 cm^{-1} region) and would be volatile above 300 °C. The stability of the supported rhenium oxide phase on alumina at 500 °C and the absence of strong Raman bands in the 160 - 200 cm^{-1} region strongly argues against the presence of rhenium oxide aggregates. Subsequent studies by Yao and Shelef employed EPR and temperature programmed reduction (TPR) to characterize the supported rhenium oxide phase [13]. They proposed that

the rhenium oxide phase supported on alumina was present as both a two-dimensional, dispersed rhenium oxide phase and a three-dimensional, crystalline rhenium oxide phase because of the two different reduction temperatures observed during the TPR experiments. More recent TPR experiments by Arnoldy *et al.*, however, demonstrated that the first reduction peak is due to the rhenium oxide surface phase and that the second reduction peak is not related to rhenium oxide, but arises from the reduction of carbonaceous residue present in the sample [17]. The TPR method is an indirect method and does not provide any information about the molecular structure of the rhenium oxide surface phase.

The first study to provide some direct molecular structural information about the surface rhenium oxide phase was the Raman study, under ambient conditions, by Kerkhof *et al.* [14]. The Raman data were found to be consistent with ReO_4 species of tetrahedral symmetry. The present Raman study also reveals that, under ambient conditions where moisture is present, the rhenium oxide exists as $[ReO_4]_{ads}$ species at all coverages, but that the ReO_4 unit is slightly distorted and possesses C_{3v} symmetry. More recent *in situ* IR studies by Nakamura *et al.* suggested that the surface rhenium oxide phase consists of $[ReO_4]_{ads}$ species of tetrahedral symmetry at low coverages and dimeric $[Re_2O_7]_{ads}$ species at higher coverages [15]. These IR studies, however, collected data only in the rhenium–oxygen stretching region, $\approx$900 - 1100 cm^{-1} and employed only perrhenate ion, ReO_4^-(aq), and crystalline Re_2O_7 as reference compounds. The inability to collect IR data below $\approx$900 cm^{-1}, due to the cut-off caused by IR absorption by the alumina support, prevents a complete structural analysis of the rhenium oxide surface phase solely from IR measurements. This problem, however, does not exist for Raman spectroscopy because the γ-Al_2O_3 support is not Raman active. These *in situ* IR studies, however, do provide data suggesting that, at low rhenium oxide loading on alumina, only one surface rhenium oxide species is present (consistent with $[ReO_4]_{ads}$), and that at high rhenium oxide loading on alumina a second rhenium oxide species is also present (possessing a more complex rhenium oxide structure).

In situ Raman studies of the rhenium oxide supported on alumina system were performed by Wang and Hall [16]. The *in situ* studies were performed by evacuating the rhenium oxide–alumina samples at 500 °C and cooling to −196 °C. The low temperature employed would be expected to give sharper Raman bands by reducing thermal broadening effects. Wang and Hall assigned the Raman bands to the presence of a monomeric rhenium oxide surface species possessing a distorted tetrahedral structure. Closer examination of Wang and Hall's Raman data reveals a somewhat more complex situation. At low rhenium oxide loading (1% Re/Al_2O_3), only one symmetric stretching mode at 1015 cm^{-1} is present, but at high rhenium oxide loading (4 - 9% Re/Al_2O_3) two symmetric stretching modes at 1015 and 1004 cm^{-1} are present. The 1015 cm^{-1} Raman band is more intense than the 1004 cm^{-1} Raman band. Thus, two different surface rhenium oxide species are present on the alumina support at high rhenium oxide coverages,

because each rhenium oxide molecular structure can give rise to only one symmetric stretching mode [25]. The close proximity of the 1015 and 1004 cm^{-1} Raman bands would prevent detection of the weaker 1004 cm^{-1} band at more elevated temperatures, room temperature or above, due to thermal broadening effects. The 9% Re/Al_2O_3 Raman spectra reported by Wang and Hall also possess additional Raman bands at 895, 800, 343 and 313 cm^{-1}. Raman data below 200 cm^{-1} were unfortunately not collected and would have provided critical information about the surface rhenium oxide molecular structure. The 1015, 895 and 343 cm^{-1} Raman bands are consistent with the presence of a dehydrated $[ReO_4]_{ads}$ surface species, and are essentially the same as those found in the present investigation during laser-induced dehydration studies at higher temperatures. The additional Raman bands at 1004, 800 and 313 cm^{-1}, however, are due to a more complex surface rhenium oxide species. A second dehydrated $[ReO_4]_{ads}$ surface species could conceivably produce a set of Raman bands at 1004, 895 and 313 cm^{-1}. This would still not account for the Raman band at 800 cm^{-1}, which occurs at a frequency significantly less than that expected for the antisymmetric stretch of the $[ReO_4]_{ads}$ species. Comparison with the rhenium oxide reference Raman spectra (see Figs. 1 and 2) suggests that the 800 cm^{-1} band is probably due to the symmetric stretch of a distorted, octahedrally coordinated surface rhenium oxide species. These additional bands may also originate from a dimeric $[Re_2O_7]_{ads}$ surface species containing one tetrahedral and one octahedral rhenium oxide unit. Such a structure is found in the solid perrhenic acid, $O_3Re{-}O{-}ReO_3(H_2O)_2$ [42]. Unfortunately the 165 - 200 cm^{-1} region, which is characteristic of the Re—O—Re bending modes, was not investigated by Wang and Hall [16]. The *in situ* Raman data of Wang and Hall suggest that, upon dehydration of high-loaded rhenium oxide on alumina, in addition to $[ReO_4]_{ads}$ there are probably other surface rhenium oxide species: a second $[ReO_4]_{ads}$, $[ReO_6]_{ads}$ or dimeric $[Re_2O_7]_{ads}$ surface species. Additional Raman studies are necessary to confirm the interesting data reported by Wang and Hall.

Edreva-Kardjieva and Andreev proposed that the surface rhenium oxide species on alumina is present as a monolayer of surface aluminum mesoperrhenate, $AlReO_5$ [18]. This conclusion regarding the molecular structure of the surface rhenium oxide arises primarily from diffuse reflectance spectroscopy studies under ambient conditions. The ability of diffuse-reflectance spectroscopy to discriminate between different surface rhenium oxide species, however, was not demonstrated by these investigators. Furthermore, $Ba_3(ReO_5)_2$ possesses the ReO_5 unit and gives rise to a strong symmetric stretch at $\approx$700 cm^{-1} in the Raman spectrum [30], and no such band was observed in any of the Raman studies. The Raman spectroscopy studies have established that rhenium oxide supported on alumina is only present as isolated $[ReO_4]_{ads}$ species under ambient conditions, and there is no evidence to support the aluminum mesoperrhenate structure.

Ellison *et al.* [19] concluded that at higher rhenium oxide loadings on alumina the three-dimensional ammonium perrhenate structure was retained

after calcination, but at low loadings surface rhenium oxide clusters were formed which possessed a perrhenate-like structure. These conclusions were drawn primarily from the results of extended X-ray absorption and fine structure (EXAFS) measurements on the Re L_3 edge. The recent TPR experiments by Arnoldy *et al.* [17], however, demonstrated that ammonium perrhenate decomposes to the rhenium oxide surface phase upon calcination at 525 °C, and the Raman measurements of Kerkhof *et al.* [14] clearly showed that only $[ReO_4]_{ads}$ is present at all rhenium oxide surface coverages on the alumina support under ambient conditions. The results of Ellison *et al.* are, however, consistent with more moderate calcination temperatures, where the ammonium perrhenate salt has been shown to be present at high loadings on the Al_2O_3 support [17].

In summary, from the present investigation and previously reported studies [12 - 19], the following conclusions can be made regarding the molecular geometry of the surface rhenium oxide species on alumina. Temperature programmed reduction experiments demonstrate that rhenium oxide on alumina is present as a surface phase [17]. This conclusion is in agreement with *in situ* IR studies which reveal that the alumina surface hydroxyl groups are removed by the supported rhenium oxide phase [12]. The sensitivity of the surface rhenium oxide Raman signal to moisture further confirms that rhenium oxide is present as a two-dimensional phase adsorbed on the alumina support surface [11, 16]. Molecular structure information about the surface rhenium oxide species is primarily obtained from vibrational spectroscopy studies. Raman spectroscopy studies reveal that under ambient conditions, where adsorbed moisture is present, the surface rhenium oxide species on alumina is present as $[ReO_4]_{ads}$ possessing C_{3v} symmetry [14, 16]. This is confirmed by XANES measurements under ambient conditions. *In situ* IR and Raman studies, which remove the adsorbed moisture, suggest that the nature of the rhenium oxide species on the alumina surface may depend on rhenium oxide loadings [15, 16]. At low rhenium oxide coverages on the alumina support surface, the surface rhenium oxide is present as $[ReO_4]_{ads}$ possessing C_{3v} symmetry [15, 16]. At high rhenium oxide coverages on the alumina support surface, the surface rhenium oxide is present as $[ReO_4]_{ads}$ as well as a second surface rhenium oxide species whose structure is not completely known at this time [15, 16]. The additional Raman bands may be due to a second $[ReO_4]_{ads}$, $[ReO_6]_{ads}$ or dimeric $[Re_2O_7]_{ads}$ surface species. *In situ* Raman spectroscopy and XANES experiments on high-loaded rhenium oxide on alumina catalysts are currently underway at our laboratories to reproduce and identify the molecular structures of these additional surface rhenium oxide species.

Acknowledgement

We thank G. Meitzner and F. W. Lytle for assistance in obtaining the XANES data. The X-ray measurements were made at the Stanford Synchrotron Radiation Laboratory, which is supported by the DOE.

References

1 Y. Murakami, M. Inomata, A. Miyamoto and K. Mori, *Proc. 7th Int. Congr. Catalysis, Tokyo, 1980*, Elsevier , Amsterdam, 1981, p. 1344.
2 F. Roozeboom, P. D. Cordingley and P. J. Gellings, *J. Catal., 68* (1981) 464.
3 W. H. Davenport, V. Kollonitsch and C. H. Kline, *Ind. Eng. Chem, 60* (1968) 10.
4 I. E. Wachs, C. C. Chersich and J. H. Hardenbergh, *Appl. Catal., 13* (1985) 335.
5 S. S. Chan, I. E. Wachs, L. L. Murrell and N. C. Dispenziere, Jr., *J. Catal., 92* (1985) 1.
6 I. E. Wachs, R. Y. Saleh, S. S. Chan and C. C. Chersich, *Appl. Catal., 15* (1985) 339.
7 Y. C. Liu, G. L. Griffin, S. S. Chan and I. E. Wachs, *J. Catal., 94* (1985) 108.
8 I. E. Wachs, R. Y. Saleh, S. S. Chan and C. Chersich, *Chemtech., 15* (1985) 756.
9 R. Y. Saleh, I. E. Wachs, S. S. Chan and C. C. Chersich, *Div. Petrol. Chem., ACS, 31* (1986) 272.
10 S. Soled, L. Murrell, I. Wachs and G. McVicker, *Div. Petrol. Chem., ACS, 28* (1983) 1310.
11 S. S. Chan, I. E. Wachs, L. L. Murrell, L. Wang and W. K. Hall, *J. Phys. Chem., 88* (1984) 5831.
12 A. A. Olsthoorn and C. Boelhouwer, *J. Catal., 44* (1976) 197.
13 H. C. Yao and M. Shelef, *J. Catal., 44* (1976) 392.
14 F. P. J. M. Kerkhof, J. A. Moulijn and R. Thomas, *J. Catal., 56* (1979) 279.
15 R. Nakamura, F. Abe and E. Echigoya, *Chem. Lett., Jap. Chem. Soc.*, (1981) 51.
16 L. Wang and W. K. Hall, *J. Catal., 82* (1983) 177.
17 P. Arnoldy, E. M. Van Oers and O. S. L. Bruinsma, *J. Catal., 93* (1985) 231.
18 R. M. Edreva-Kardjieva and A. A. Andreev, *J. Catal., 94* (1985) 97.
19 A. Ellison, A. Bickerstaffe, G. Diakun and P. Worthington, *J. Mol. Catal., 36* (1986) 67.
20 I. E. Wachs, F. D. Hardcastle and S. S. Chan, *Spectrosc., 1* (1986) 30.
21 B. M. Kincaid and P. M. Eisenberger, *Phys. Rev. Lett., 34* (1975) 1361.
22 J. Jaklevic, J. A. Kirby, M. P. Klein, A. S. Robertson, G. S. Brown and P. M. Eisenberger, *Solid State Commun., 23* (1977) 679.
23 E. A. Stern and S. M. Heald, *Nucl. Instrum. Methods, 172* (1980) 397.
24 F. W. Lytle, R. B. Greegor, E. C. Marques, D. R. Sandstrom, G. H. Via and J. H. Sinfelt, submitted to *J. Catal.*
25 K. Nakamoto, *Infrared and Raman Spectra of Inorganic and Coordination Compounds*, Wiley, New York, 3rd edn., 1978.
26 E. B. Wilson, J. C. Decius and P. C. Cross, *Molecular Vibrations: The Theory of Infrared and Raman Vibrational Spectra*, Dover Publications, New York, 1980.
27 F. Gonzalez-Vichez and W. P. Griffith, *J. Chem. Soc., Dalton Trans.*, (1972) 1416.
28 R. A. Johnson, M. T. Rogers and G. E. Leroi, *J. Chem. Phys., 56* (1972) 789.
29 J. Hauck and A. Fadini, *Z. Naturforsch., 256* (1970) 422.
30 E. J. Baran and A. Müller, *Z. Anorg. Allg. Chem., 368* (1969) 168.
31 B. Jezowska-Trzebiatowska, J. Hanuza and M. Baluka, *Spectrochim. Acta, 27A* (1971) 1753.
32 I. R. Beattie and G. A. Ozin, *J. Chem. Soc. (A)*, (1969) 2615.
33 J. M. Stencel, L. E. Makovsky, T. A. Sarkus, J. DeVries, R. Thomas and J. A. Moulijn, *J. Catal., 90* (1984) 314.
34 J. M. Stencel, L. E. Makovsky, J. R. Diehl and T. A. Sarkus, *J. Catal., 95* (1985) 414.
35 S. S. Chan and I. E. Wachs, *J. Catal., 103* (1987) 224.
36 E. Payen, S. Kasztelan, J. Grimblot and J. P. Bonnelle, *J. Raman Spectrosc., 17* (1986) 233.
37 H. Knözinger, *Adv. Catal., 16* (1976) 179.
38 H. Knözinger and P. Ratnasamy, *Catal. Rev. Sci. Eng., 17* (1978) 31.
39 J. A. Horsley, I. E. Wachs, J. M. Brown, G. H. Via and F. D. Hardcastle, *J. Phys. Chem., 91* (1987) 4014

40 F. W. Kutzler, C. R. Natoli, D. K. Misemer, S. Doniach and K. O. Hodgson, *J. Chem. Phys.*, *73* (1980) 3274.
41 J. Wong, F. W. Lytle, R. P. Messmer and D. H. Maylotte, *Phys. Rev.*, *B30* (1984) 5596.
42 H. Beyer, O. Glemser and B. Krebs, *Angew. Chem.*, *80* (1968) 286.